Aero-elastic loads on a 10 MW turbine exposed to extreme events selected from a year-long Large-Eddy Simulation over the North Sea

Gerard Schepers[1], Pim van Dorp[2], Remco Verzijlbergh[2], Peter Baas[2], Harmen Jonker[2]

[1]TNO Energy Transition, Wind Energy, Petten, 1755LE, The Netherlands
[2]Whiffle, Delft, 2629JD, the Netherlands

Correspondence to: J.G Schepers (Gerard.schepers@tno.nl)

Abstract. In this article the aero-elastic loads on a 10 MW turbine in response to unconventional wind conditions selected from a year long Large Eddy Simulation on a site at the North Sea are evaluated. Thereto an assessment is made of the practical importance of these wind conditions within an aero-elastic context based on high fidelity wind modelling. Moreover the accuracy of BEM based methods for modelling such wind conditions is assessed. The study is carried out in a joint effort by the TNO Energy Transition and the Dutch meteorological consultancy company Whiffle.

Notations

BEM	Blade Element Momentum
DEL	Damage Equivalent load
DOWA	Dutch Off-shore Wind Atlas
FVW	Free Vortex Wake
RWT	Reference Wind Turbine
TKE	Turbulent kinetic energy
TI	Turbulent intensity
LLJ	low-level jet

1 Introduction

This article describes a study in which the loads are assessed as calculated on a 10 MW wind turbine in response to extreme wind events on the North Sea. The turbine on which the loads are calculated is the 10 MW Reference Wind Turbine as designed in the EU project AVATAR (Sieros, et al., January 2015).

The study is carried out within the Dutch national project DOWA in a cooperation between ECN part of TNO and Whiffle. The extreme wind events have been selected from a year-long simulation with the operational LES code GRASP from Whiffle (Gilbert, et al., 2019). GRASP is an atmospheric LES model nested in a global weather model which allows the detailed modelling of meteorological phenomena on a spatial and temporal grid resolution which is fine enough for aero-elastic load

calculations. The resulting extreme wind events are then fed as wind input to the aero-elastic solver PHATAS from WMC (now LM) as used by TNO Energy Transition (Lindenburg, 2005). PHATAS is coupled to the AeroModule which is a code with two aerodynamic models, a Blade Element Momentum (BEM) method and a Free Vortex Wake (FVW) method AWSM (Boorsma, Grasso, & Holierhoek, 2012). The calculated loads as response to these extreme wind events are compared with the loads from a reference design load spectrum which is available from the AVATAR project (Stettner, et al., April 2015) This reference design load spectrum is calculated with a conventional procedure along the IEC standards. By comparing the loads in response to the extreme events with those from the conventional design load spectrum, the importance of extreme wind events can be assessed for practical (load) purposes.

The structure of the present article is as follows:

- In section 2 the goal of the study is explained.
- In section 3 a short description is given of the turbine on which the load calculations are performed. It also describes the location where the turbine is located.
- Section 4 describes the load modelling of extreme wind events. It explains the GRASP model and the selected extreme events with the validation using measurements. It also describes the rotor modelling from PHATAS and AeroModule and the interface between PHATAS and GRASP.
- Section 5 describes the calculation of the reference design load spectrum.
- In section 6 the comparison between the loads from the extreme events and those from the reference spectrum is given together with an evaluation of results. Special attention will be given to the analysis of results at an extreme low-level jet, since these events are often believed to have significant impact on turbine loading, see e.g. (Duncan, November 2018)
- Finally, in section 7 the conclusions and recommendations are given.

2 Goal

The goal of the present study is defined as:

- To demonstrate the coupling between the LES code GRASP and the aero-elastic code PHATAS; GRASP delivers the wind input to PHATAS as an alternative to the default wind modelling commonly used in aero-elastic load modelling which is based on stochastic wind field methods
- To assess the impact of extreme wind events on the load spectrum of a representative 10 MW turbine. These extreme events are selected from a year-long GRASP simulation. The loads are compared with those from a standard design load spectrum as calculated by PHATAS in a conventional way along IEC standards. In this way it can be assessed whether these extreme events yield loads that deviate significantly from the design load spectrum. This can thus be seen as a proof-of-concept study to explore the merits of using high-fidelity wind simulations as input for load

calculations. Such site-specific simulations could someday be done more routinely in wind turbine and wind farm design and could eventually lead to a rethinking of the use of standard design load spectra.

- To assess the accuracy of a standard BEM model for the calculation of the selected extreme wind events. Thereto the loads as calculated by a BEM model are compared with those from a higher fidelity code free vortex wake method AWSM.

Hence it should be realized that, apart from demonstrating the combined GRASP-PHATAS tool, the research aims to investigate the impact of extreme events on the load spectrum but also the accuracy of a standard BEM model for the calculation of these events. These are two different subjects which are to some extent unrelated. However the second subject is a spin-off from the first subject in view of the fact that are calculations are performed with AeroModule which is a code based on two different aerodynamic models: A BEM based model and a higher fidelity FVW model. So insights on the accuracy of BEM are automatically obtained.

3 Reference turbine and location

The turbine on which the investigations are carried out is the AVATAR Reference Wind Turbine (RWT) (Sieros, et al., January 2015). This is a turbine with a rated power of 10 MW as designed in the EU project AVATAR. This project was carried out from 2013 until the end of 2017. AVATAR was coordinated by ECN(TNO) and it had a consortium of 13 partners, including GE and LM as industrial partners.

The AVATAR RWT is a low induction variant of a 10 MW RWT which was designed in another EU project, INNWIND.EU (Bak, et al., 2013). The INNWIND.EU RWT has a diameter of 178 meter. The low induction concept used in the AVATAR RWT makes an increase in rotor diameter possible to D= 205.8 meter with a limited increase in loads. The hub height of the AVATAR RWT is 132.7 meter by which the lowest point of the rotor plane is at an altitude of 29,8 meter and the upper part of the rotor plane is at 235,6 meter.

The rated rotor speed is 9.8 rpm which leads to a tip speed of 103.4 m/s;

All design data (the aerodynamic and aero-elastic data of blades, tower, shaft and other components) of the AVATAR RWT are publicly available (Sieros, et al., January 2015).

A controller is designed which below rated wind speed, aims for maximum power production with variable rotor speed operation using a speed dependent generator torque setpoint (for optimum tip speed ratio) and constant optimal blade pitch angle. Above rated wind speed, the rotor speed and generator power are regulated to their nominal rating using constant generator torque and collective blade pitch control.

Moreover the design load spectrum has been calculated (Stettner, et al., April 2015). This design load spectrum will be used

as reference to the loads as calculated in response to the extreme events from GRASP. The calculations of the design load spectrum have been repeated with the most recent versions of design tools to assure consistency in tools, see section 5.

The site where the turbine is placed is the location of the Meteorological IJmuiden (MMIJ) in the North Sea, 85 km offshore from the Dutch shore (N52°50.89' E3°26.14'). Hence, it is this location where the wind input is calculated by the Whiffle code GRASP.

The mast is shown in Fig. 1 and the instrumentation of the mast is given in (Werkhoven & Verhoef, 2012). Measurements are taken with anemometers on a mast which are placed at three different heights above sea level, i.e.: 27m, 58m and at the top level of 92 meter (note that some wind speed sensors are mounted at an altitude of 85 meters as well).

They are combined with LIDAR measurements which are taken at 90, 115, 140, 165, 190, 215, 240, 265, 290, 315 meter above sea level.

Figure 1: Meteorological Mast IJmuiden

4 Calculation of loads for extreme events

4.1 Wind input

4.1.1 Grasp

The GRASP code is a Large Eddy Simulation (LES) model developed by Whiffle that is based on the Dutch Atmospheric Large Eddy Simulation (DALES). The LES code runs on Graphics Processing Units (GPUs) and is therefore referred to as

GRASP: GPU-Resident Atmospheric Simulation Platform. GRASP can be run with boundary conditions from a large scale-
115 weather model (Gilbert, et al., 2019) For this study, GRASP has been run for the location of the Meteo Mast IJmuiden in the Dutch North Sea area with boundary conditions from the ERA5 reanalysis dataset (Hersbach et al., 2020) that provides global data of historical atmospheric and ocean conditions. Driving the LES with boundary conditions from a large-scale weather model, ensures that the full spectrum of atmospheric flow from synoptic to turbulent scales is considered. Amongst others, the interaction between atmospheric stability, turbulence and shear is resolved.

120 A full year of LES runs of 24 hours each (i.e. 365 simulations of 24 hours, plus a 2-hour spin up period for each simulation) has been performed on a resolution of 20m. For reference, Fig. 2 presents a comparison between modeled and observed 92-m wind speed for the entire year.

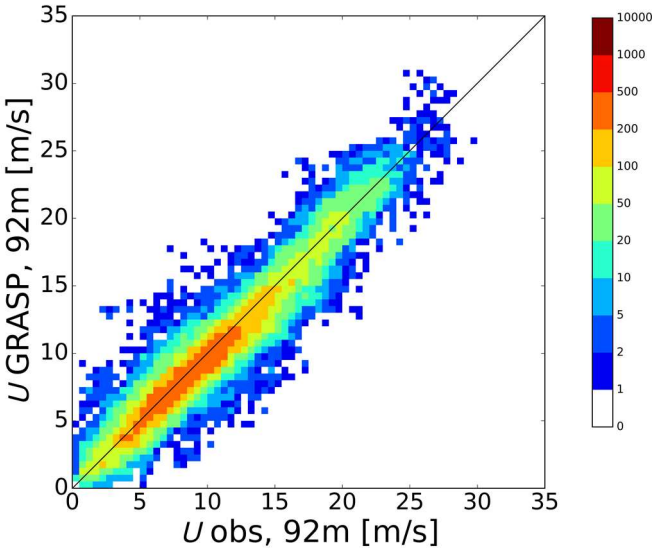

Figure 2: Scatter-density plot of modeled versus observed 92-m wind speed.

125

From this year of model simulations, several types of extreme wind events have been identified, including low-level jets, high shear, high veer, strong gusts, fast ramps and high turbulence cases. These cases have been re-run and used as boundary conditions for a higher resolution run in the concurrent precursor setting. To this end, a three-way nested simulation has been carried out, see Fig. 3, at 8, 4, and 2 meter resolution with 256 grid boxes in each direction which gives a domain size of 2x2
130 km^2, 1x1 km^2 and 500x500 m^2 respectively. The finest grid with a resolution of 2 meter yields 51 wind speed points over the 103 meter AVATAR blade radius. The finest temporary resolution is 10 Hz which yields an azimuth interval of 6 degrees at the rated rotor speed of 10 rpm (which is in the order of intervals used in aero-elastic simulations). The computation time of the year of LES runs on 20m resolution amounts to roughly 2 days on a cluster with 4 NVIDIA Volta GPUs plus some

additional runtime for the selected high-resolution runs. The chaotic character of the wind field in Fig. 3 illustrates the realistic representation of atmospheric turbulence in the model.

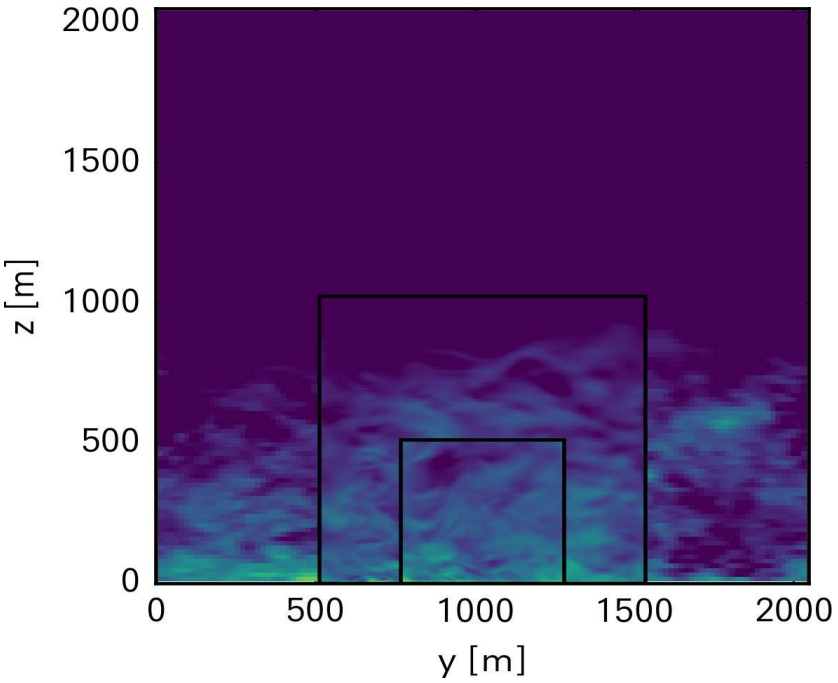

Figure 3: Vertical cross-sections of wind speed in the three different nested LES runs. The coarsest runs use periodic lateral boundary conditions and large-scale forcing from ERA5. The higher resolution runs use lateral boundary conditions from the 'upper' nests.

4.1.2 Selection and validation of extreme events

The GRASP simulations were carried out from 2014/12/1 to 2015/12/1. The calculation domain of the nested simulations was centered around the hub height of 133 meters with a spatial resolution of 2 meters and a temporary resolution of 0.1 seconds as mentioned in section 4.1.1. The considered wind speeds are between 5 and 25 m/s i.e. between the cut-in and cut-out wind speed of the AVATAR RWT

Then the following five "extreme" cases of 10 minutes were selected.

- Strongest low-level jet (LLJ). Note that LLJ's were detected with the algorithm from (Baas, 2009)
- Strongest wind veer over the rotor
- Strongest shear over the rotor
- Highest turbulence kinetic energy (TKE) below cut-out wind speed
- Highest turbulence intensity (TI) around rated wind speed (i.e. higher than 10 m/s) and lower than cut-out

Figure 4 presents an overview of the selected extreme wind cases. For each extreme wind case (columns), profiles of wind speed, U, wind direction, phi, turbulence intensity, TI, and turbulent kinetic energy, TKE, are shown (rows). For comparison, also the MMIJ observations and ERA5 reanalysis data are added. Although the significance of a one-to-one comparison of modeled and observed 10-minute records is limited, especially when considering extreme events, clear correspondence between the model results and the observations is observed. In Section 4.1.3 the modeled extreme events are discussed from a climatological point of view.

For the strongest low-level jet, Fig. 4 shows that the wind speed at the lowest point of the rotor plane is approximately 9.2 m/s. Going upward it increases to a maximum value of almost 13 m/s. This value is reached slightly below hub height. Then above hub height the wind speed decreases to approximately 10.3 m/s at the upper part of the rotor plane. The wind speed variation with height goes together with a relatively large veer from approximately 230 degrees at the lowest point of the rotor plane to 239 degrees slightly below hub height above which it remains more or less constant. It must be noted that a shear exponent of 0.2 (i.e. the exponent used in the IEC reference load spectrum, see section 5) at a comparable hub height wind speed of 13 m/s yields a velocity of 9.7 m/s at the lower part of the rotor plane. In other words, the shear prescribed by the standards is only slightly less than the shear from the LLJ in the lower part of the rotor plane. For the selected LLJ case the corresponding observed wind profile does not show a jet-like profile. In Section 4.1.3 it will be shown that on a climatological basis modeled and observed low-level jets have similar characteristics.

The strongest wind veer case shows a wind direction of approximately 85 degrees at the lowest part of the rotor plane and a wind direction of approximately 120 degrees at the upper part, leading to a wind direction difference of 35 degrees. The correspondence with observations is reasonable. Note that for this strong veer case but the observed and modeled wind speed profile show a clear LLJ.

The strongest shear case shows a wind speed of approximately 11.5 m/s at the lowest part of the rotor plane above which it increases to almost 16 m/s at hub height above which it increases further to approximately 19 m/s at the upper position of the rotor plane. The observations show a comparable wind shear. Although a wind speed difference of 8.5 m/s over the rotor plane is seemingly large it must be noted that a wind shear exponent of 0.2 (i.e. the exponent prescribed in the standards for the normal operating condition cases) and a hub height wind speed of 16 m/s already gives a wind speed difference of 6.2 m/s over the rotor plane.

For the case with extreme turbulence intensity and extreme turbulent kinetic energy the turbulence intensities at hub height are found to be approximately 5% and 6.5% at approximately 14.8 m/s and 22.5 m/s respectively. It is noted that although these turbulence intensities are the highest for the selected year, they are much lower than the values for turbulence class A at the corresponding wind speeds (approximately 18% and 16%). This indicates that the reference design load spectrum as calculated in the AVATAR project is conservative for isolated turbines at the selected site. However even a turbulence class C (the lowest possible turbulence class in IEC) leads to turbulence intensities which are still far above the extreme

185 turbulence intensities in the selected year.

It is also important to note that the extreme shear and extreme low-level jet cases go together with very low turbulence levels. This is shown in table 1, which gives the turbulence intensity as function of height for the LLJ event.

Height [m]	Turbulence intensity [%]
31	5.8
81	3.3
133	1.6
185	1.3
235	1.2

190 Table 1: Turbulence intensity as function of height for the extreme low-level jet case

The turbulence intensity at hub height is 1.6%. This low turbulence intensity should be kept in mind when analyzing the load results. The turbulence intensity decreases from 1.6% at hub height to 1.2% at h = 235 meter despite the decreasing wind speed above hub height in Fig. 2. This implies that the decreasing turbulence intensity with height should be attributed to a
195 strong decrease in standard deviation of wind speed fluctuations which overcompensates the decreasing wind speed. In fact, this is what can be expected under the strongly stratified conditions that favor the formation of LLJs. In contrast, for the LLJ case the observed values of TI do increase with height, which would be much harder to explain. Note that estimating turbulence quantities from LiDAR observations is not trivial, see e.g. Sathe at al. (2011).

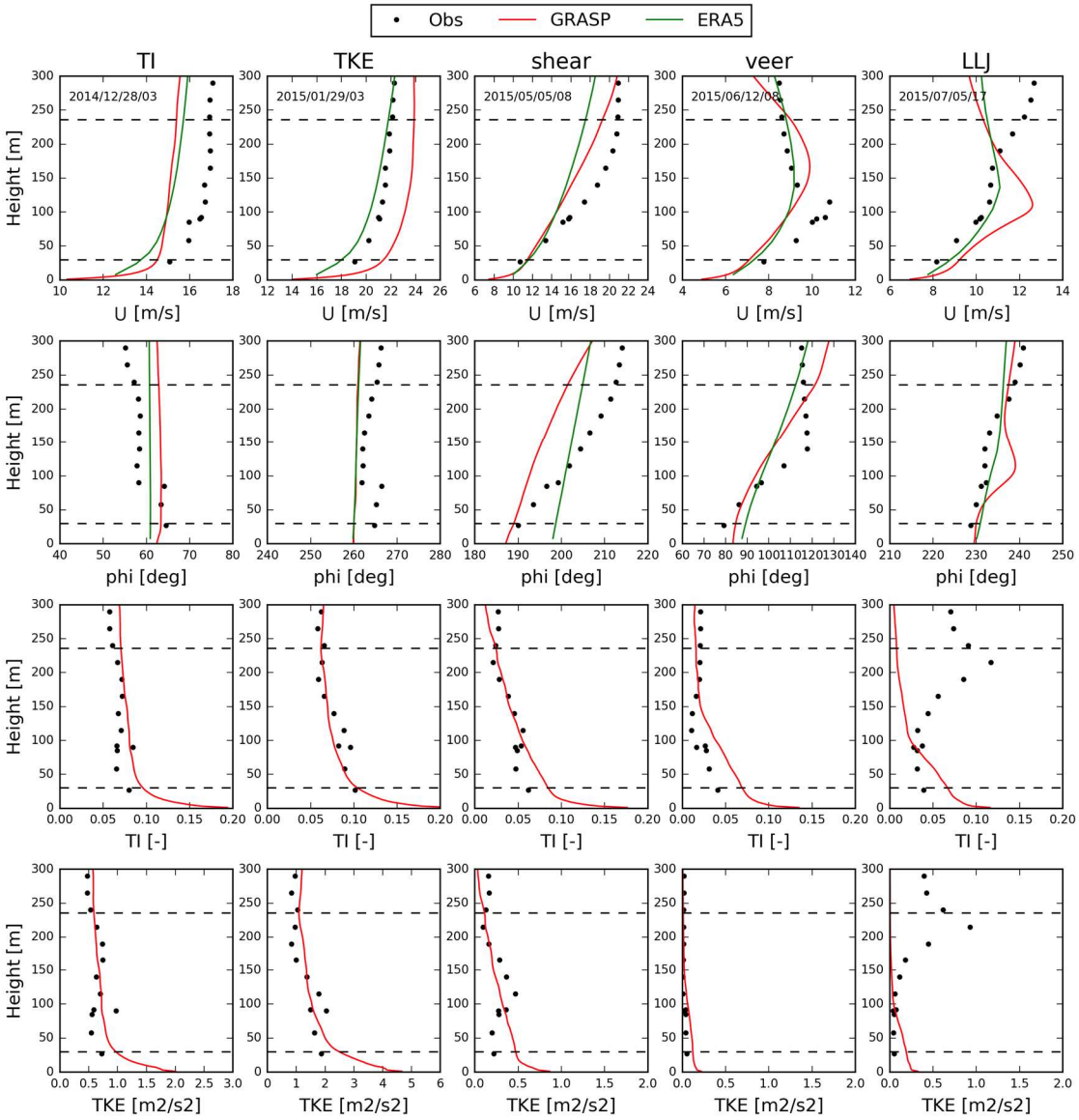

Figure 4: Profiles of four meteorological quantities (wind speed U, wind direction phi, turbulence intensity TI and turbulent kinetic energy TKE) for the five selected extreme cases (different columns) with high TI, TKE, wind shear, veering, and a strong LLJ. Observations are indicated as black dots, the high-resolution GRASP (2m grid-spacing) results in red, and ERA5 reanalysis data in green. Dashed lines indicate the upper and lower part of the rotor plain.

4.1.3 Climatology of extreme events

Instead of a one-to-one comparison of isolated 10-minute records, here we compare the climatology of extreme wind events from the GRASP LES and the observations.

Fig. 5 shows profiles of wind speed and veering with height for the 90th percentile of strongest shear and veer conditions between 215 and 90 m. For strong shear conditions (left) the GRASP and ERA5 wind speed profiles are close to the observations. For these cases the wind direction changes only weakly with height and is slightly larger in the observations than in the model. For strong veer conditions (right) the wind speed is weak and constant with height above roughly 90 m. The strong veering of the wind with height is well-represented by GRASP and underestimated by ERA5.

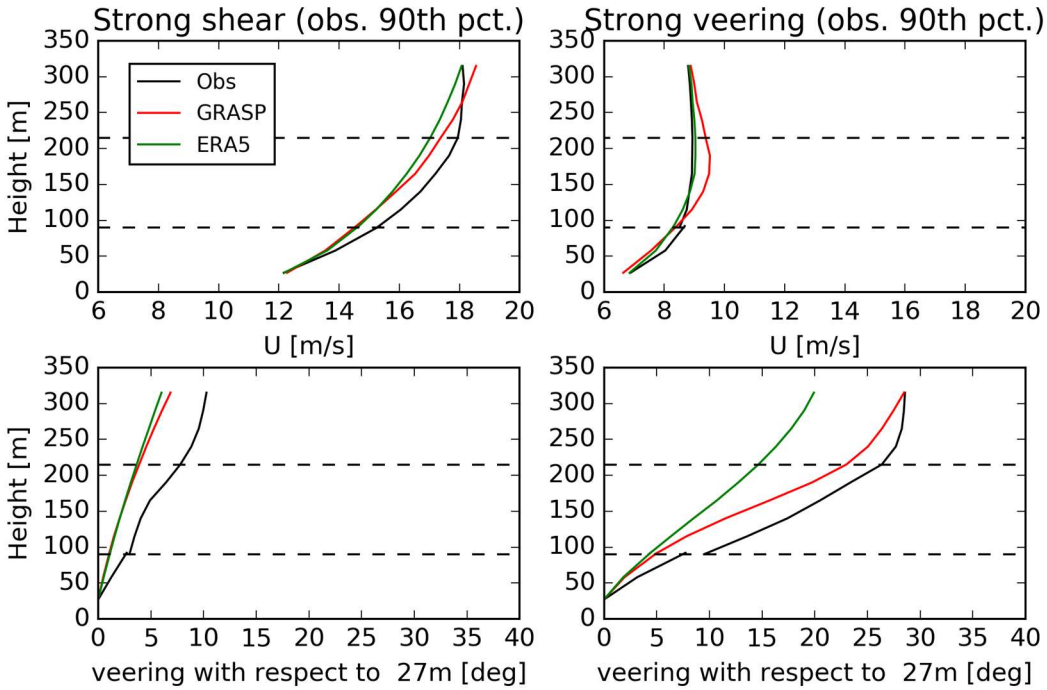

Figure 5. Comparison of the 90th percentile strongest shear (left) and veer (right) conditions from observations, ERA5 and GRASP.

In Fig. 6 the standard deviation of the wind is plotted versus the wind speed for the 92-m level. The top panels include one year of observations and simulations. The division of these two quantities gives the TI. For reference, lines of equal TI of 5% and 10% are indicated. Clearly, stronger winds yield more intense fluctuations. The model tends to have slightly higher TI values than observed, but the difference is within a few percent. For wind speeds of around 10 m/s, the observed and modeled TI values are mostly close to 5%.

In section 6 of this paper, it will be shown that the loads from the LLJ are relatively low. The low loads at LLJ are partly caused by the very low turbulence intensities which go together with an LLJ. It is then important to know whether these low

turbulence intensities at LLJ's are also found in the measurements. Therefore, the lower panels of Fig. 6 only include data points that satisfy the criterion for the occurrence of a low-level jet. Clearly, TI values of LLJ events are generally in the range of 2% (sometimes even less than 1%) at an altitude of 92 meter which is seen as a confirmation that low turbulence intensities are found at LLJ events indeed

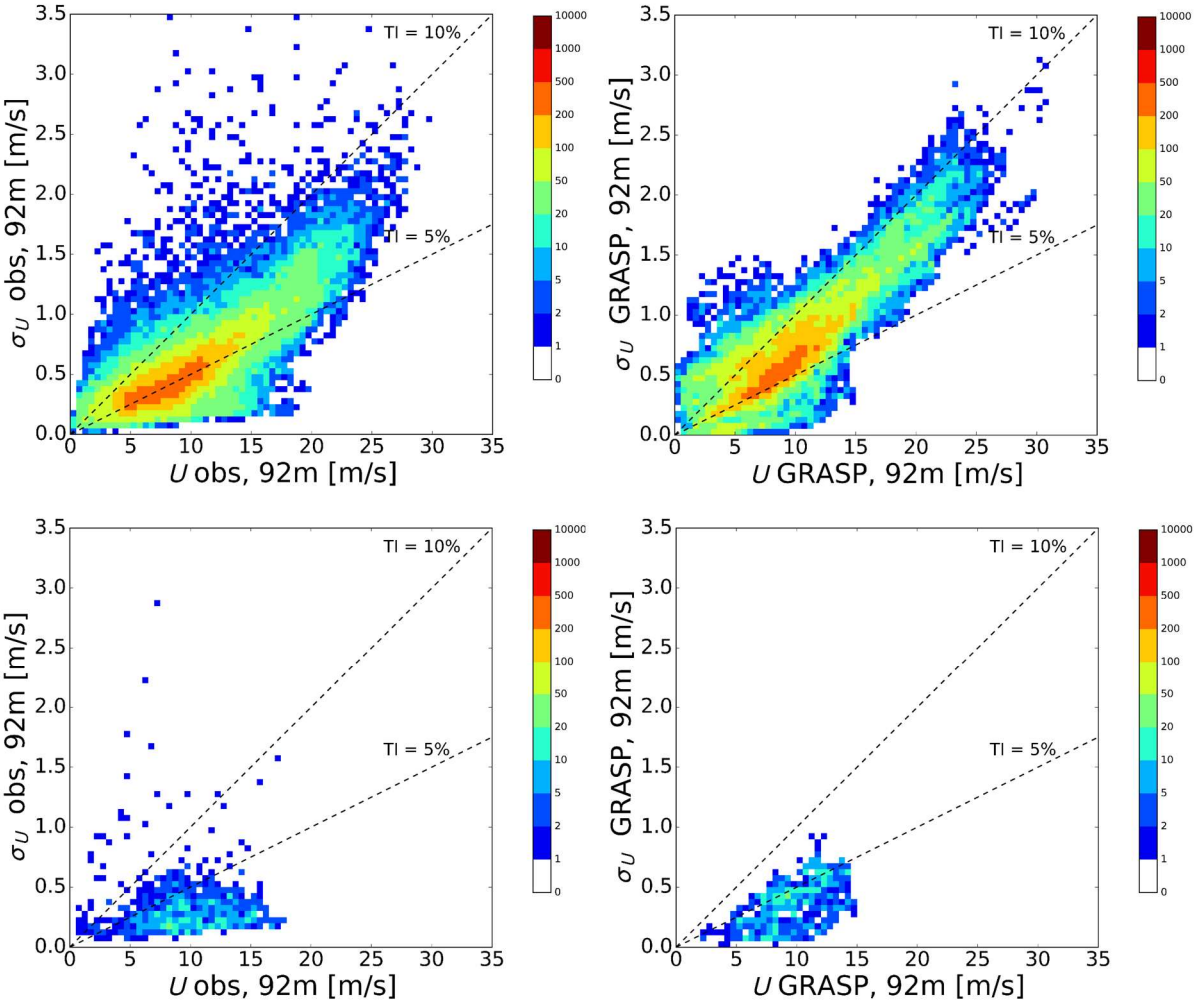

Figure 6 : Scatter-density plot of the standard deviation of the wind speed versus the wind speed at the 92-m level. Left panels: observations; right panels: model results, Top panels: entire year; lower panels: only LLJ cases.

Fig. 7 shows average low-level jet wind speed profiles for the observations, GRASP, and ERA5, i.e. the profiles averaged over all timestamps of the respective dataset when a LLJ was present according to the LLJ criterion (Baas et al, 2009). The agreement between GRASP and the observations is very good. ERA5 underestimates the speed of the LLJ. The frequency of

LLJ occurrence is highest in the observations with 4.8 % of the 10-minute records. For GRASP and ERA5 the LLJ frequency amounts to 2.3% and 0.6%, respectively.

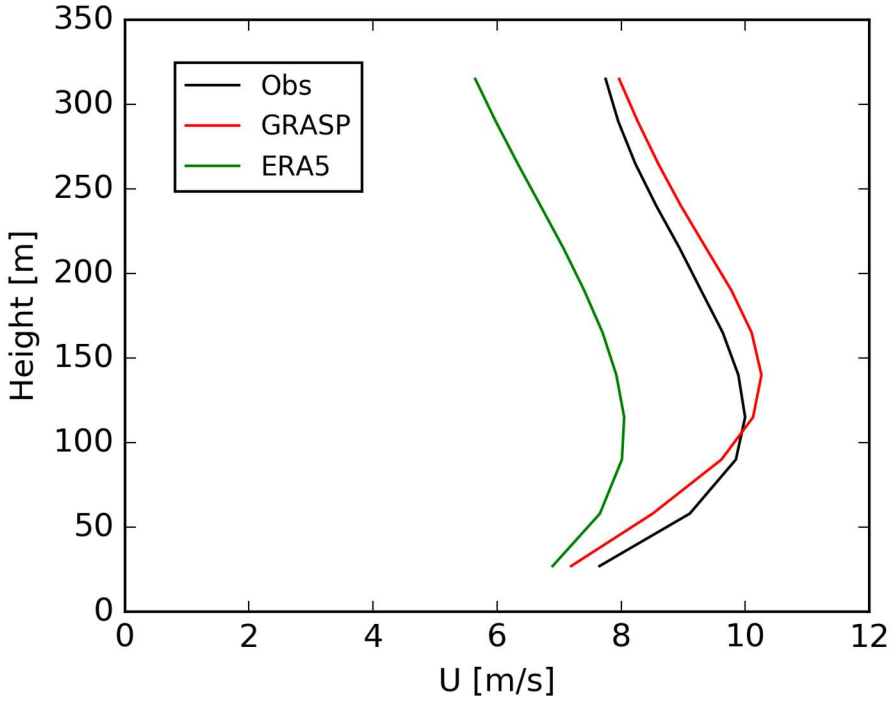

Figure 7: Average low-level jet wind speed profiles.

4.1.4 Concluding remarks on validation

In summary, the extreme wind cases that were selected based on GRASP model output, represent 'real weather'. That is to say, there is a strong qualitative and often quantitative agreement between the modelled and observed extreme events of LLJ, wind shear, veer, TI and TKE. Although the agreement for the selected LLJ is moderate, it is encouraging to see that many other LLJ events in the year of simulation find a shear which is comparable to the measurements. Moreover, most LLJ's go together with low turbulence levels and large veer in both calculations and measurements. In general, the climatology of the extreme events (shear, veer, TI, TKI and LLJ) as modeled by GRASP resembles the observed extreme events well.

4.2 Aero-elastic modelling of GRASP extreme events

The aero-elastic loads in response to the extreme GRASP cases from section 4.1.2. are calculated with the PHATAS code (Lindenburg, 2005). The development of this code started in 1985 by ECN (now TNO) but later the code has been transferred to WMC (now LM). The code takes into account blade flexibilities in all three directions (flatwise, edgewise and torsional) but also tower and drive train flexibilities. Also, the control of the AVATAR turbine is taken into account.
The default aerodynamic solver of PHATAS is based on the Blade Element Momentum (BEM) theory. This is an efficient but lower fidelity model which, because of its efficiency is used for industrial design calculations. In its basis such BEM model is steady and 2D, by which phenomena like yaw and stall are calculated with a very large uncertainty. Therefore, in the last decades several engineering models have been developed which are added to the BEM theory. These engineering add-ons cover phenomena like unsteady and 3D effects as well as yaw and stall. They are still of a simplified efficient nature which makes them suitable for industrial calculations. These engineering models are validated and improved with the most advanced measurement data (Schepers J. G., November 2012) and with high fidelity models (Schepers J.G. et al, 2018)
Although the default aerodynamic solver of PHATAS is based on the BEM theory, the GRASP events are calculated with a PHATAS version which is linked to an alternative aerodynamic solver AeroModule as developed by ECN part of TNO. AeroModule is a code which has an easy switch between an efficient BEM based model and a high fidelity but time consuming FVW based model AWSM (Boorsma, Grasso, & Holierhoek, 2012) which allows a straightforward comparison of these two models with precisely the same input. In this way it can be assessed how well the load response is calculated with a BEM model in comparison to the load response as calculated from the higher fidelity model AWSM.
In the present study the blade root flatwise moment is considered. Both extreme loads and the Damage Equivalent fatigue Loads (DEL) are considered with a Wohler slope of 10. It is noted that the Damage Equivalent Load translates the underlying rain flow cycle spectrum into a single number. This facilitates the presentation of results, but it conceals the underlying frequency information from the rain flow cycle spectrum. The loads are calculated in the coordinate system from Germanischer Lloyd.
The computation time of the load calculations is much faster than real-time for BEM on a simple laptop. The Free vortex wake calculations are a factor 100-1000 slower (dependent on number of wake points and the wake cut-off length etc).

4.3 Interface between GRASP and PHATAS

The input for AeroModule (and so PHATAS) consists amongst others of the 3D wind speeds at several locations in the rotor plane as function of time. For the present study they were supplied by Whiffle in separate files in NETCDF format in the resolution which is given in section 4.1.1. They were transformed by ECN part of TNO into TurbSim wind simulator files (Jonkman, 2009).

It is noted that the turbine yaw angle is fixed and aligned with the time averaged wind direction at hub height from the GRASP wind input.

5 Calculation of reference design load spectrum

The reference design load spectrum for the AVATAR RWT has been calculated and assessed in (Stettner, et al., April 2015). It is calculated along the IEC standards for wind class IA, which was considered representative for offshore conditions by the AVATAR consortium. As mentioned before this is a conservative turbulence class for the present location.

The load spectrum from (Stettner, et al., April 2015) is based on an almost complete set of design load cases, i.e. normal production (DLC 1.2), standstill, stops etc. In the present study it is only the normal production cases from DLC 1.2 which are repeated. In section 6. it will be shown that these cases are sufficient for the present assessment and there is no need to include special cases.

The reference load cases are carried out as 10-minute time series for mean wind speeds ranging from 5-25 m/s, with a wind speed interval of 2 m/s, a shear exponent of 0.2, where the wind input is generated from the stochastic wind simulator SWIFT using 6 different seeds. A small yaw angle of 8 degrees is included to account for yaw control tracking errors.

It is noted that the aerodynamic model with which the reference spectrum is calculated is based on the default BEM model of PHATAS where the GRASP events from section 4 are calculated with both BEM and FVW. Apart from fundamental model differences between BEM and FVW all calculations are carried out in exactly the same way, with the same degrees of freedom, engineering models used etc., in order to assure consistency in results.

6. Comparison between aero-elastic loads at extreme events with loads from the reference spectrum

Figure 8 shows the resulting equivalent fatigue flatwise moment as function of the 10-minute averaged wind speed from the reference design load spectrum and extreme GRASP events. The values indicated with *reference* are the loads as calculated for DLC1.2. They are compared with the BEM and AWSM calculated loads for the case of extreme low-level jet (*LLJ*), Veer, Shear, Turbulence Intensity (*TI*) and Turbulence kinetic energy (*TKE*).

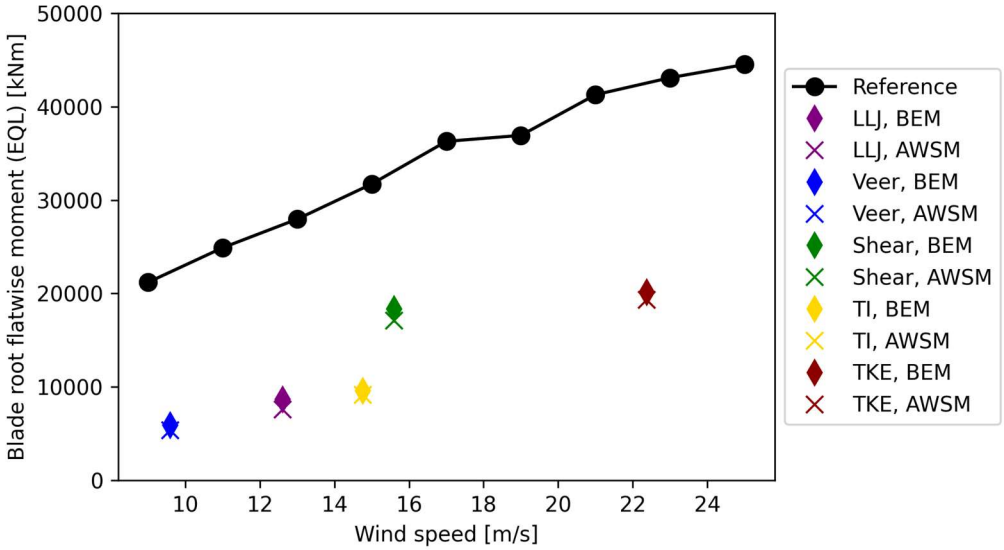

Figure 8: Equivalent blade root flatwise moment: DLC1.2 versus GRASP extreme wind events

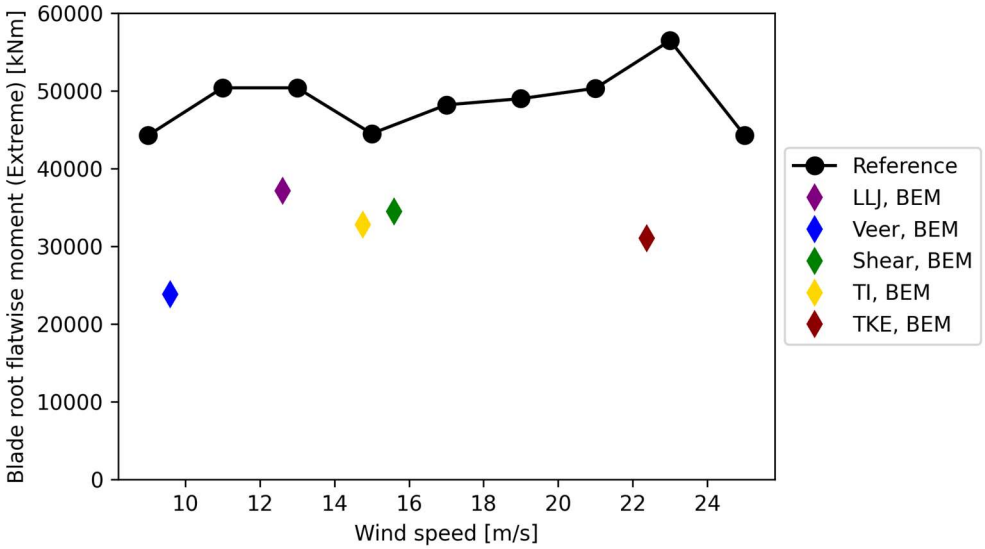

305

Figure 9: Extreme blade root flatwise moment: DLC1.2 versus GRASP extreme wind events.

In Fig. 9 the extreme flatwise moment as extracted from the 10-minute time series is compared and again plotted as function of wind speed. The extreme load has been extracted for a BEM based calculation only. The presentation of extreme loads as

function of wind speed is strictly speaking non-sensical since it is the overall maximum value which is determinant. This way of presenting is chosen because it shows the wind speed where the extremes are found.

The following remarks can be given on the presentation:

- In all cases the extremes were found to be the maximum positive values (using the sign conventions from the GL coordinate system).
- The present analysis is based on normal production cases (DLC 1.2) only which means that special and extreme load cases are excluded. As such the actual maximum extreme load from a full IEC spectrum could even be higher than the values presented in Fig. 9. Some indication for that is found in (Savenije, et al., December 2017) which shows that often non DLC 1.2 cases (e.g. DLC 6.2, idling at storm loads) are more extreme indeed. However, in the sequel it will be shown that even the extreme loads from DLC 1.2 are higher than the loads from the extreme GRASP events by which there was no use to calculate the non-DLC1.2 load cases.
- The design load spectrum has been calculated for 6 different seeds per wind speed. The results from Fig. 8 is based on the averaged equivalent load. The values from Fig. 9 values are the overall extremes per wind speed.
- In order to gain some further understanding on the results, the loads from the low-level jet are analyzed in more detail. Thereto table 2 presents the DEL of the flatwise moment for the low-level jet from BEM and AWSM in the third and fourth row respectively. In the second row the corresponding DEL from DLC1.2 is given for a wind speed of 13 m/s which is very close to the 10-minute averaged hub height wind speed at the low-level jet. In the second column the DEL is calculated (which correspond to the results from Fig. 8).

The third column gives the DEL from the azimuthally binned averaged variation. This azimuthally binned averaged variation is (for a linear system) similar to the deterministic variation which is mainly a result of the shear (although the veer in the LLJ event and the 8 degrees yaw error for DLC 1.2 leads to a deterministic variation as well). The equivalent loads from the deterministic variation are calculated for the BEM results only.

	$M_{flat,\ DEL}$ [Nm]	$M_{flat,\ DEL}$ deterministic [Nm]
DLC1.2(BEM), 13 m/s	27955000	15904000
LLJ(BEM)	8661000	8584700
LLJ(AWSM)	7602100	

Table 2: Comparison of equivalent blade root flatwise moment for extreme low-level jet

335

6.1 Assessment of loads from extreme events

A very important conclusion is that the loads in response to the extreme wind events from GRASP remain within the load envelope of the reference spectrum. This is true for the equivalent fatigue loads, see Fig. 8, which shows that all DEL's from the GRASP extreme events are lower than the DEL's from the reference DLC 1.2 at comparable wind speeds. It is also true
340 for the extreme loads, see Fig. 9. As explained above the "real" extreme reference loads are likely to be even higher than the values given in these figures, since the results in these figures consider DLC 1.2 only. This makes that the extreme loads from the GRASP wind events remain even more within the reference spectrum.

From table 2 it can be concluded that the equivalent flatwise moment at the LLJ is only 31% (approximately) of the equivalent load from DLC 1.2. Some explanatory remarks to this observation can be made:

345

- As mentioned in section 4.1.2 the turbulence level at the low-level jet is extremely low (approximately 1.6 % at hub height) where the turbulence level for DLC1.2 at 13 m/s is in the order of 19%. The very low turbulence level at the LLJ explains, at least partly, the much lower fatigue load. This is confirmed by the DEL of the deterministic variation in the third column which is almost similar (99%) to the DEL of the total variation in the first column. The 1%
350 difference is the addition from turbulence and should be compared with the difference between deterministic and total variation from DLC 1.2 which is approximately 43%. This indicates how little the low turbulence level at the LLJ adds to the fatigue loads.
- Still the DEL of the deterministic variation at the LLJ is much lower (approximately 54%) than the DEL of the deterministic variation at DLC 1.2. This indicates that the low fatigue loads at a LLJ are not only caused by the lower
355 turbulence levels but it is also the different shear from the LLJ which lowers the DEL. Some further explanation is offered by Fig. 10. This shows a comparison between the azimuthally binned averaged flatwise moments for the LLJ and DLC1.2. Azimuth angle zero indicates the 12 o'clock position. The rotor rotates clockwise so azimuth angle 90 indicates the 3 o'clock position when looking to the rotor. The variation from DLC 1.2 has a 1P variation with a relatively large amplitude. This is the behavior of the flatwise moment in an atmosphere with 'common' vertical wind
360 shear. The wind speed (and so the loads) decreases when the blade rotates from the vertical upward 12 o'clock (zero azimuth) position to the vertical downward 6 o'clock (180 azimuth). The flatwise moment increases again when the blade rotates from 180 degrees towards 360 degrees.
- The azimuthal variation in flatwise moment from the low-level jet is very different from the variation which results from DLC1.2. It shows a 2P variation with a relatively small amplitude. This 2P variation can be explained with the
365 LLJ wind speed profile from Fig. 4 which shows the wind speed to be low at 0 degrees azimuth (the 12 o' clock position, when the blade is pointing vertical upward) and at 180 degrees (the 6 o'clock position, when the blade is pointing vertical downward). The wind speed is maximum at (approximately) hub height which correspond to azimuth angles of 90 and 270 degrees (i.e. the 3 o' clock and 9 o' clock position when the blade is standing

horizontally). This velocity variation is reflected in the flatwise moment. It is low at 0 degrees, high at (roughly) 90 degrees and 270 degrees and low again at 180 degrees. This leads to a 2P variation, but the load amplitude is relatively small. Hence, although the 2P load variation happens twice as often as the 1P load variation from the DLC 1.2. the lower amplitude of the variations leads to a lower fatigue.

- It is noted from Fig. 4 that the present LLJ has a maximum velocity close to hub height and it could be argued that a different hub height leads to a different load behavior. The lowest part of the rotor plane of the AVATAR RWT is at an altitude of 29.8 meter and the upper part is at an altitude of 235.6 meter. It was not considered feasible to decrease the tower height and lower the rotor plane even more. Also, a lowering of hub height would bring the maximum in LLJ wind speed even closer to hub height (See Fig. 4). Therefore, an increase of tower height has been investigated but this was limited by the domain size of the GRASP field which extends up to a maximum altitude of 255 meter. Hence the tower height cannot increase with more than 19.4 meter. A hub height of 250.7 meter has been investigated but this did not lead to significantly different conclusions (i.e. the loads from the LLJ remain within those of the reference spectrum)

6.1 Accuracy of calculating loads from extreme events

From figure 8 and table 2 it can be concluded that the DEL of the blade root flatwise moment is overpredicted with the BEM model (assuming that the fatigue loads as calculated with the FVW model AWSM are close to reality). Similar observations were made in (Boorsma, Chasapogianis, Manolas, Stettner, & Reijerkerk, September 2016) and (Boorsma, Wenz, Aman, Lindenburg, & Kloosterman, September 2019) where differences are reported in the order of 10-20% for load cases which are representative to IEC normal production. The present study shows overpredictions which are in the same order of magnitude i.e. 14% for the extreme LLJ, 11% for the extreme veer case, 7% for the extreme shear case but only 4-5% for the extreme turbulence intensity and turbulent kinetic energy. The difference between AWSM and BEM based fatigue shaft loads (not shown in this paper) were generally found to be smaller and less straightforward than for the blade root flatwise moment: in some cases, AWSM even predicts higher fatigue loads than BEM.

The commonly believed explanation for the overpredicted BEM DEL lies in a more local tracking of the induced velocity variations in FVW models, by which they vary synchronously with the variation in inflow. This synchronization then damps out the variations in angle of attack. Moreover, FVW models allow for a more intrinsic and realistic modelling of shed vorticity variations in time.

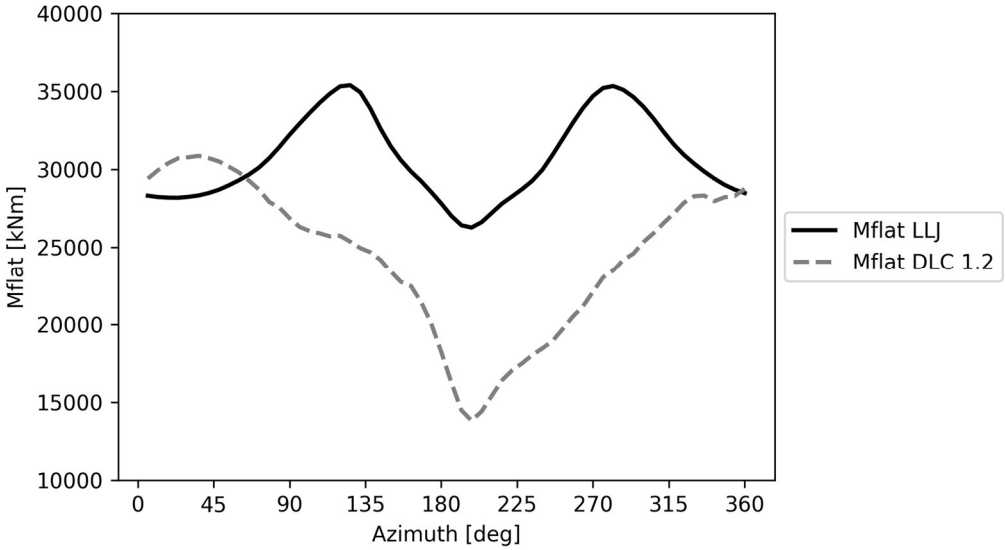

Figure 10 Azimuthally binned averaged flatwise moment: LLJ versus DLC1.2

7 Conclusions and recommendations

- A successful coupling has been established between the LES wind field model GRASP from Whiffle and the aero-elastic code PHATAS (with AeroModule) from ECN part of TNO. Thereto extreme events, including a low-level jet are selected from a 1-year simulation of GRASP wind fields. These events are fed as wind input files to the PHATAS code and used to simulate the AVATAR 10 MW Reference Wind Turbine (RWT) at an offshore location.
- A validation of the LES Wind fields has taken place by comparing the calculations with measurements from Meteorological Mast IJmuiden. This validation shows that there is generally a good agreement in the load determining characteristics of the LES wind fields by which the calculated events can be used with confidence to assess the importance of them in an aero-elastic load context. However, more validation is needed, in particular on turbulence characteristics at high altitudes (say higher than 100 meter)
- The resulting (DEL and extreme) loads for the selected events are (roughly speaking) 30-70% lower than those from the reference design load spectrum of the AVATAR RWT. As such, the often-heard expectation that low-level jets have significant impact on loads is not confirmed for the present offshore situation. This is partly explained by the very low turbulence intensities which go together with the LLJ. However, the deterministic DEL from the LLJ shear is also lower than the deterministic DEL from DLC 1.2. This is due to the fact that the shear from the LLJ is not very extreme in comparison to the shear from the IEC standards. The LLJ shear profile then leads to a 2P variation instead of a 1P variation from ‘normal shear’ but the amplitude is smaller resulting in a lower fatigue damage. From the

results one could hypothesize that the combination of the shear and turbulence levels from the IEC standards may often lead to conservative loads. However much more research is needed to warrant a conclusion, especially in the validation of the on-site turbulent wind fields.

- It is noted that the present LLJ has, more or less by coincidence, a maximum velocity close to hub height. A study on different hub heights didn't show a very different outcome but the limited domain size of the LES wind field made that the hub height could not increase with more than 20 meters. A study with a much taller tower (and so an extended domain size) is recommended.
- For the selected extreme events the DEL from the more physical AWSM model are considerably lower than the DEL of BEM model which indicates that BEM overpredicts fatigue loads. The difference is largest for the shear driven cases and for a rigid construction. Efforts should be undertaken to improve the BEM fatigue calculations for such shear events.
- The present research can be considered as a proof-of-concept study to investigate the potential of a coupling between turbine response models and high-fidelity wind models. The success of it leads to the recommendation to explore such coupling even further for the calculation of a full design load spectrum. This makes it possible to assess the validity of a conventional method for the calculation of a design load spectrum based on stochastic wind simulators. The higher fidelity of the present method makes that eventually design calculations could be based on physical wind models. Future work should focus on applying and validating this method in more challenging case studies, such as in full-scale wind farms where the down-stream turbulence is heavily affected by the turbines themselves. Including other wind turbines in the LES domain also has the benefit that the implicit assumption that the upstream turbulence is not affected by the turbine can be overcome. Finally, we recommend to also study situations where turbines are situated in complex terrain environments.
- Although the coupling between PHATAS and GRASP was very successful the interfacing through GRASP output and PHATAS wind input files can be improved. Ideally an integrated approach should be developed without the need of interface files.

Author contributions. J.G. Schepers assembled and ran the load simulation results and analyzed the overall results. P. van Dorp and H.J.J. Jonker modified the LES code and performed the GRASP simulations. R.A. Verzijlbergh assisted in the analysis of the results. P. Baas performed the validation of the GRASP simulations

Acknowledgement The research was sponsored by the Topsector Energy Subsidy from the Ministry of Economic Affairs and Climate; F. Savenije (ECN part of TNO) is acknowledged for the calculation of the reference load spectrum. K. Boorsma (ECN part of TNO) is acknowledged for his support on the AeroModule code.

Competing interests. The authors declare that they have no conflict of interest.

Bibliography

Baas, P. B. A climatology of nocturnal low-level jets at Cabauw. *Journal of Applied Meteorology and Climatology, 48(8),*, 1627-1642, 2009

Bak, C., Zahle, R., Bitsche, R., Kim, T., Yde, A., Henriksen, L., . . . Natarjan, A. *The DTU 10 MW Reference Wind Turbine.* Danish Technical University, 2013.

Boorsma, K., Chasapogianis, P., Manolas, D., Stettner, M., & Reijerkerk, M. *Comparison of models with respect to fatigue load analysis of the INNWIND.EU and the AVATAR RWT.* Deliverable D4.6 of the EU project AVATAR, September 2016.

Boorsma, K., Grasso, F., & Holierhoek, J. *Enhanced approach for simulation of rotor aerodynamic loads.* Energy Research Center of the Netherlands, ECN-M-12-003, 2012.

Boorsma, K., Wenz, F., Aman, M., Lindenburg, C., & Kloosterman, M. *TKI WOZ VortexLoads final report.* TNO 2019 R11388, September 2019.

Duncan, J. *Observational Analyses of the North Sea low-level jet* . TNO R11428, November 2018 .

Gilbert, C., Messner, J. W., Pinson, P., Trombe, P. J., Verzijlbergh, R., van Dorp, P., & Jonker, H. (2020). Statistical post-processing of turbulence-resolving weather forecasts for offshore wind power forecasting. Wind Energy, 23(4), 884–897. https://doi.org/10.1002/we.2456

Hersbach, H., Bell, B., Berrisford, P., Hirahara, S., Horányi, A., Muñoz-Sabater, J., … Thépaut, J. N. (2020). The ERA5 global reanalysis. *Quarterly Journal of the Royal Meteorological Society*, 146(730), 1999–2049. https://doi.org/10.1002/qj.3803

Jonkman, B. *TurbSim User Guide.* NREL/TP-500-46198, 2009.

Lindenburg, C. *PHATAS Program for Horizontal Axis Turbine Analysis and Simulation.* Energy Research Center of the Netherlands, ECN, ECN-I-05-005, 2005.

Sathe, A., Gotschall, J., & Courtney, M. *Can Wind Lidars measure turbulence.* Journal of Atmospheric and Oceanic Technology, Volume 28, July 2011.

Savenije, F., Gonzalez Salcedo, A., Martin San Roman, R., Lampropoulos, N., Barlas, A., Sieros, G., . . . Maeder, T. *Evaluation of the new design, The advanced Reference Wind Turbine.* Deliverable 1.7 of the EU project AVATAR, December 2017.

Schepers, J.G. *Final Report of the EU project AVATAR.* http://www.eera-avatar.eu/fileadmin/avatar/user/AVATAR_final_report_v26_2_2018.pdf, 2018 (Accessed December 17, 2019).

Schepers, J. G. *Engineering models in Wind Energy Aerodynamics.* TUDelft, PhD thesis, November 2012.

Sieros, G., Lekou, D., Chortis, D., Chaviaropoulos, P., Munduate, X., Irissarri, A., . . . Reijerkerk, M. *Design of the AVATAR RWT rotor.* Deliverable D1.2 of the EU project AVATAR, January 2015.

Stettner, M., Irissari Ruiz, A., Madsen, H., Verelst, D., Croce, A., Sartori, L., . . . Reijerkerk, M. *Evaluation and cross-comparison of te AVATAR and INNWIND.EU RWT's.* Deliverable D1.3 of EU project AVATAR April 2015

Werkhoven, E., & Verhoef, J. *Offshore Meteorological Mast IJmuiden.* Energy Research Center of the Netherlands, ECN-Wind-Memo 12-010, 2012.

490

495